Measurement of Gearbox Surface Frequency Response Functions for HUMS Algorithm Improvement

Daniel R. Wade
US Army Aviation Engineering Directorate
Redstone Arsenal, AL 35898

Christopher G. Larsen
Etegent Technologies Ltd
Cincinnati, OH 45212

Abstract

Vibration diagnostic algorithms used to identify incipient bearing faults are installed in Digital Source Collectors (DSC) on nearly 2000 US Army rotorcraft. These algorithms depend on the structural vibration characteristics of the bearings, gearboxes, and mounting brackets to transmit the signatures associated with bearing abnormalities and faults. Two distinct algorithm families exist to measure changes in these signatures: the broadband spectral energy family and the demodulation family. Each of these uses the unique vibration signatures associated with the natural frequencies and transfer paths of the monitored bearings. The Aviation Engineering Directorate has estimated the Frequency Response Function for each of the monitored bearings from 5 to 50 kHz using a piezo-exciter mounted directly to the gearboxes at the bearing load zones and measured by the appropriate DSC accelerometer. The testing for this effort was completed on six airframes: the Apache AH-64D, the Black Hawk UH-60L and MH-60M, the Chinook MH-47G and CH-47D, and the Kiowa Warrior OH-58D. This paper details the three-phase effort showing the entire process including the validity of the measurements and samples of the FRF estimates.

Introduction

To date, the US Army has installed nearly 2000 Digital Source Collectors, or DSCs, on rotorcraft to monitor the health of gearboxes, hanger bearings, and swashplate bearings. Over the last decade, these installations have been completed for all the rotorcraft platforms in the inventory, to include the Black Hawk (MH and UH-60 A, L, and M), the Apache (AH-64 A and D), the Kiowa Warrior (OH-58D), and the Chinook (CH-47D). Installation of the DSCs is forecast to continue during the next several years, until the fleet is fully equipped. This initiative has given Army engineers the opportunity to fine tune the built in vibration diagnostics of the DSCs thus enabling Condition Based Maintenance (CBM).

Engineers in the Dynamics Branch of the Aviation Engineering Directorate have focused on the ability of the vibration-based diagnostics to predict the failure of bearings throughout the drive train. This would include hanger bearings, swashplate bearings, and internal gearbox bearings. There are two distinct families of detection algorithms used on Army DSCs: broadband spectral energy, and demodulation energy. Furthermore, these two families also include *peak pick* methodologies that report the amplitude of a single spectral line. The focus of this paper will be on the improvement of these

two algorithm families through the measurement of actual gearbox physical characteristics.

Previous algorithm performance improvement has focused on individual cases of gearbox or bearing failures monitored by DSCs already installed on aircraft in the field and directly associated with damage through the Army Tear-Down Analysis (TDA) process (1). This method of single component, single algorithm improvement works well when monitored components fail frequently, however the high reliability of the great majority of components installed on Army aircraft limits this method of algorithm improvement. Many of the monitored components have never been effectively monitored by a DSC during failure. This is caused by lost DSC data and the inefficiencies in the Army supply system which is not currently designed to deal with the demands of the growing CBM efforts.

Algorithm Behavior

Army DSC bearing diagnostics are designed to detect spalling which is the most common bearing failure mechanism. This is achieved by two different algorithms: Broadband Root Sum Squared (RSS) Energy and Amplitude Demodulation (AMD). Each of these algorithms operate on the time domain signal of an installed accelerometer that is excited by the bearing defect as each of the rolling elements pass by or inversely as a spalled rolling element contacts the inner or outer race. Each algorithm is then employed to detect the impulse generated at the spall site.

The RSS algorithm operates on the simple assumption that the impulse created at the spall initiation point excites the structure attached to the bearing, which in turn responds to the impulse by resonating. The resonances that are excited by the impulse are thus a function of the quality and amplitude of the impulse. The RSS sums together the spectral lines associated with the modes of the gearbox. In the past, tuning this algorithm was simply a process of observing field faults or failures.

RSS operates on the complex conjugate of the FFT of the windowed and averaged time domain signal. It has input arguments to assign the overall band width as well as any small bands within the overall bandwidth that need to be zeroed out. The act of removing spectral lines is usually associated with gearbox strong tones that always appear in the frequency domain. A prime example would be a gear mesh frequency. RSS can be accomplished for multiple bands on the same bearing and thus can be customized based on the uniqueness of each bearing/gearbox combination (2).

The AMD algorithm demodulates the band-passed time domain signal around a carrier frequency, where the modulation is caused by the natural resonances of the supporting structure interacting with the impulses. The assumption for this analysis is that the periodic impulses created by the bearing defect will excite the *high frequency* resonances of the gearbox or bearing housing thus allowing the algorithm to pick out exactly which portion of the bearing is failing based on the bearing geometry and speed of the inner race. For the purposes of this paper, high frequency resonances are any resonances above the normal operating frequencies of the gearbox, to include the harmonics of the gear mesh frequencies. In a typical rotorcraft gearbox, these frequencies start between 5 and 10 kHz. In certain situations (swashplate bearings), high frequency could be as low as 2 kHz.

AMD and RSS performance depend completely on the structural response of the monitored gearbox. The majority of bearing diagnostics on board Army aircraft are not optimized based on the structural response of the associated

gearboxes. The Apache fleet is the most advanced as of today because it has the largest associated ground truth data set based on a large number of completed TDAs. The purpose of this effort is therefore to increase the effectiveness of the bearing diagnostics by measuring the actual structural response associated with all the bearings that are monitored by the installed DSCs.

Phase I: Frequency Response Function Estimation with Piezo Exciter

Impulse response is a widely used method for estimating the Frequency Response Functions (FRF) of a structure. This is typically measured by an installed accelerometer and reference impulse created by an instrumented hammer. Unfortunately, instrumented hammers do not have good broadband excitation capabilities since they are typically rated up to 3 or 4 kHz. For the case of gearbox bearing diagnostics, the structural response characteristics must be measured above 20 to 30 kHz; this lead to the choice of piezoelectric devices for structural excitation.

The choice of excitation signal was very important for making good quality measurements. Piezo actuators are driven with a command signal from a function generator or acquisition system source card, and this command signal must be amplified, generally by an amplifier designed specifically for piezoelectric elements. Driving noise into a piezo element for excitation spreads the available power from the amplifier over the entire spectrum, and the power driven at any given frequency is very low. This can be illustrated as follows. Assume that the amplifier has available power P. A signal's power in a given frequency band can be calculated by integrating the PSD over that frequency band, as shown in the following equation (3).

$$P = \int_{f_1}^{f_2} S(f)\,df$$

Therefore, if the amplifier's power is spread evenly over 50 kHz, the available power-per-Hz will be 1/50,000 the total available power. This would provide inadequate force input into the system and the measurements would be very poor.

Driving a fixed frequency can provide all the available power from the amplifier at that frequency, and this provides the best signal-to-noise ratio possible; additionally, the selected frequency can be driven for as long as desired, permitting significant averaging. This is called stepped-sine excitation. The FRF amplitude and phase can be estimated using only a 2-channel oscilloscope, and if amplitude is the only interest it could even be done with calibrated RMS values from a volt meter. The obvious downside for this method is that this must be repeated for each desired spectral line, and this can be very time consuming.

An excellent alternative to stepped-sine excitation is a chirp. A five-second chirp swept from 0 – 50 kHz was chosen to provide the best balance between testing speed and accuracy. The actual source used was a VXI E1445a card – this is essentially a typical function generator in a VXI 'C-size' card. This card does not generate a true continuously-swept sine; it discretely steps through the frequencies – the desired frequency band is divided into 800 discrete frequencies, so for a 50 kHz sweep, the frequency interval is 62.5 Hz, which is more than fine enough for the larger general FRF trends that will dictate frequency-band selection. This effect is easily viewed when looking at the recorded force, as the amplitude steps slightly with frequency. While this does technically create a (very low level) step response as the source steps through the frequencies, both input and response are measured, so the FRF

computation is unaffected. A typical force measurement example is shown in Figure 1.

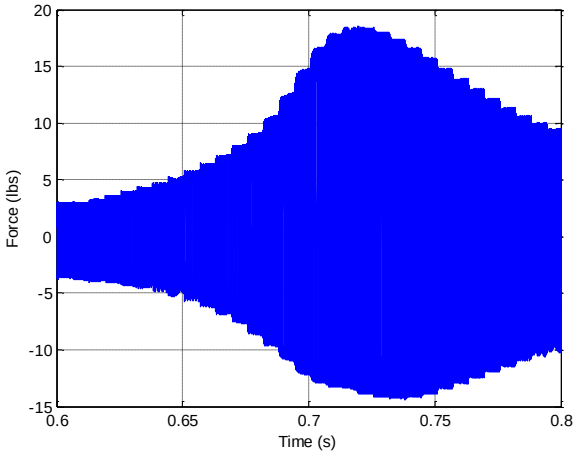

Figure 1. Discrete Swept Sine – Force Measurement

In order to get the most accurate measurement of the bearing FRFs, the best practice would be to initiate a seeded fault for each bearing to be monitored. This is obviously cost prohibitive and thus a solution that allows surface measurement of the FRFs on installed gearboxes would be the best choice. This assumes however that surface measurement of the FRF is an accurate representation of the true internal path. The first phase of this work therefore focused on the validity of this assumption using an Apache intermediate gearbox (IGB) in a lab environment.

The duplex ball bearing of the IGB was disassembled and one rolling element was removed. Part of the cage was notched to provide clearance for the piezo-exciter as shown in Figure 2. The surface of the outer race was ground slightly to permit the piezo element to sit flat on the surface and the outer race was notched slightly to provide clearance for the wires as shown in Figure 3.

Figure 2. Removal of One Bearing Element

Figure 3. Raceway Notch for Exciter

Piezo wafers (5x5x2 mm PhysikInstrumente PL-055) were wired to shielded coaxial cable and glued to the bearing outer race, with a tungsten-carbide sphere for the reaction mass. Tungsten-carbide was chosen, as it is roughly twice as dense as steel, which allowed a 2.0 gram, ¼ inch diameter sphere to fit inside the bearing. The assembled reaction-mass exciter was glued to the outer race Figure 4.

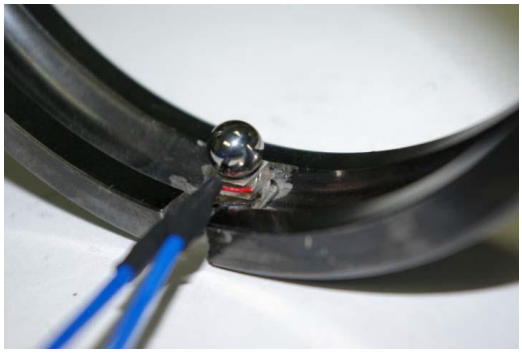

Figure 4. Installation of Exciter

The cage was placed into the outer race with one of the split inner race pieces with some epoxy to prevent the bearing from accidentally turning and damaging the exciter. The other inner race piece was epoxied in place and the instrumented bearing was installed in the gearbox as shown in Figure 5 and Figure 6. The final setup is also shown in Figure 6 where the gearbox was instrumented with six high frequency accelerometers (PCB 352A60) and the two DSC accelerometers (Dytran 3062A1 and Chadwick-Helmuth 4177B). An example comparison between external and internal excitation can be seen in Figure 7.

Figure 5. Completed Bearing Assembly

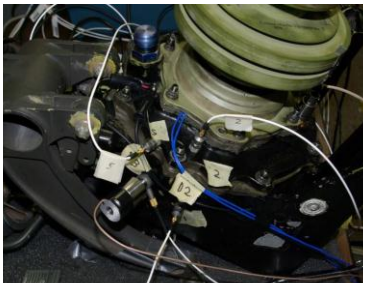

Figure 6. Completed Test Rig Assembly

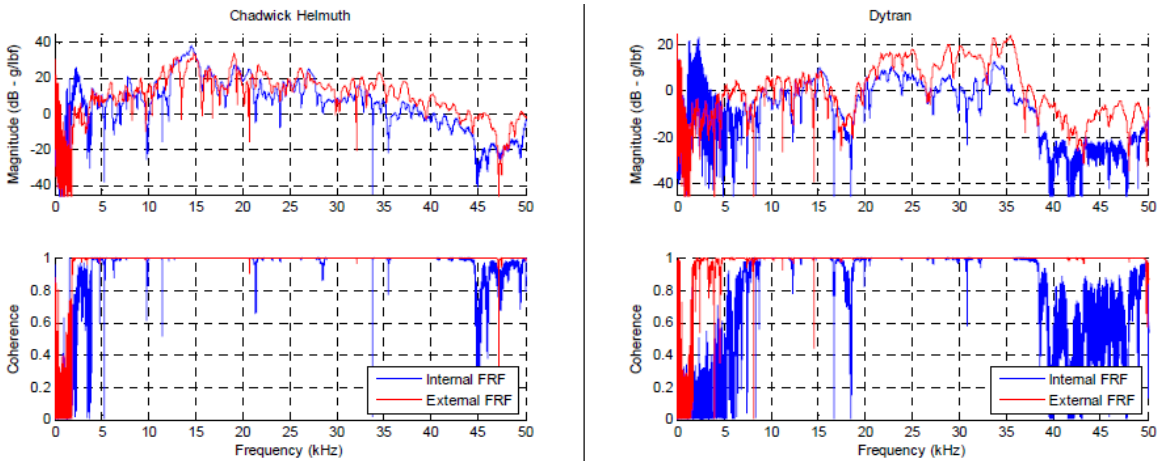

Figure 7. Example Comparison – Internal and External FRFs

Internal and external excitation of the bearings produces the same overall system response. Good agreement exists across all the sensor locations with levels of broadband attenuation being a function of location rather than frequency. This of course is the desired result when trying to simplify such a measurement to be made across a fleet of aircraft. Coherence values for these measurements are noticeably high except at low frequencies, where the exciter is not capable of producing large enough force outputs. This is because the piezoelectric exciters are of the reaction-mass type; force is inversely proportional to the square of frequency. To overcome this poor coherence,

the authors supplemented the testing with traditional impact tests at each of the locations.

Pre-Test Considerations

One area of concern with this type of transducer is crosstalk between the excitation piezo element and the force-measurement piezo element, as this would seriously corrupt the FRF estimate.

To test the level of electrical crosstalk, two piezos were mounted in close proximity to one another using an alligator-clip fixture, as shown in Figure 8. The two piezos were separated by approximately 0.1 mm, which is the thickness of the mica used to separate and insulate the piezos from each other on assembly.

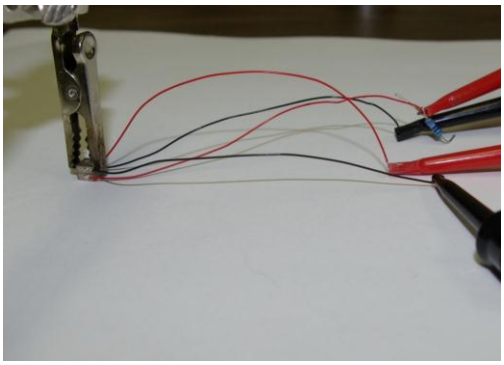

Figure 8. Piezo Element Cross-Talk Test Setup

A 0 – 50 kHz chirp was used for excitation to one of the piezos, generated by the VXI E1445a card, and this was amplified by the ISI amplifier. The voltage of the un-driven piezo was measured, and the power spectrum is shown in Figure 9. The red trace shows the crosstalk of the current setup, the green trace shows the improved system, (discussed below), and the black trace shows the noise floor (no commanded voltage to the driving piezo element). The blue trace shows a typical measurement for comparison. Note that the force measurement power is more than four orders of magnitude higher than the crosstalk amplitude throughout the frequency range.

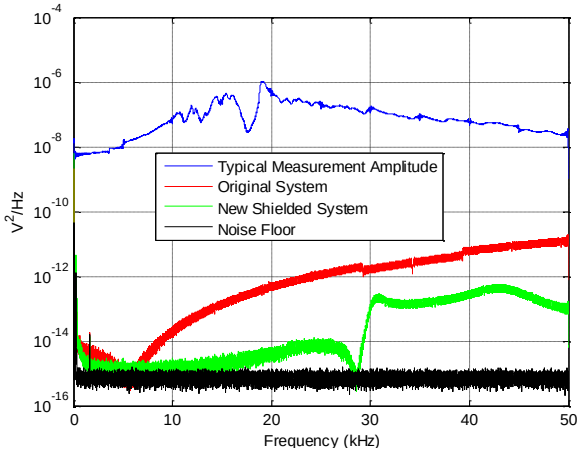

Figure 9. Crosstalk Power Spectra

As this crosstalk rises with frequency, it was assumed that it is electrical interference between the long unshielded test leads. The test leads were shortened as much as possible, to a few millimeters, and soldered to shielded coaxial cables. For further testing and easier handling, one of the piezos was potted onto a ¾ in stainless-steel hexagon. This is shown in Figure 10.

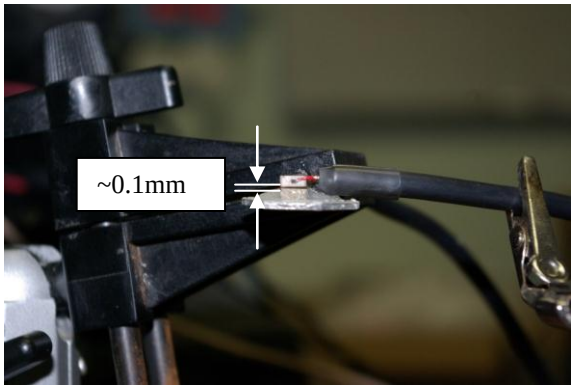

Figure 10. Piezo Crosstalk Test Setup

Preload of the Exciter

Preload was effectively tested during the repeatability tests because multiple test operators installed the exciter during these tests and

preload was not measured which would likely result in many different preload values. The consistency between those tests demonstrated that relatively small changes in preload do not affect the measurement repeatability.

FRF Processing Techniques

Sixty seconds of data were collected for each test – this provides twelve complete chirps and twelve averages. The FRFs were processed such that the block size matches the chirp length, using a uniform window (i.e. no window), and no overlap processing. Because the blocks repeat with the chirps, this satisfies the Discrete Fourier Transform (DFT) assumption that the signal is repeated infinitely before and after the block being transformed (4), eliminating the possibility of leakage and the need for a window. In fact, the chirp does not have to be triggered with the acquisition system, because the block can begin somewhere in the middle of a chirp and still repeat itself. Periodicity of the DFT can be shown from the definition of the DFT itself:

$$X_{k+N} \equiv \sum_{n=0}^{N-1} x_n e^{\frac{-2\pi i}{N}(k+N)n} = \sum_{n=0}^{N-1} x_n e^{\frac{-2\pi i}{N}kn} e^{-2\pi i n} = \sum_{n=0}^{N-1} x_n e^{\frac{-2\pi i}{N}kn} = X_k$$

Exciter Mounting Technique

Because these measurements were made on in-service helicopters (meaning that the aircraft were scheduled for five days of testing each, but modifications which inhibit an immediate return to service were not permissible), there were severe limitations as to how sensors and the shaker could be mounted. Obviously, drilling and tapping holes was not an option. Therefore, the methodology used for the testing procedure had to be demonstrated to produce meaningful, repeatable results.

It is generally assumed that a threaded mount is the only way to make high-frequency structural measurements, and for good reason. Threaded mounts would seem to provide the most rigid, repeatable means of attaching transducers and sensors to a structure. However, most desired test locations on these gearboxes have no tapped hole, and it wasn't feasible to machine a flat surface and tap a hole in those locations for this testing. Therefore, it was necessary to test the effects of mounting the sensors with an adhesive.

For this test, a scrap aluminum block was drilled through and tapped 10-32 for mounting both the piezo-exciter (Piezomechanik) with load cell (PCB 201B02) and the high-frequency accelerometer (PCB 352A60). These were screwed to the block, a 5 second 0 – 5 Volt, 0 – 50 kHz chirp was commanded to the exciter, and 30 seconds of time data was recorded. FRFs were produced in post-processing. Figure 11 shows the piezo-exciter-side of the test setup, and Figure 12 shows the high-frequency accelerometer-side of the test setup.

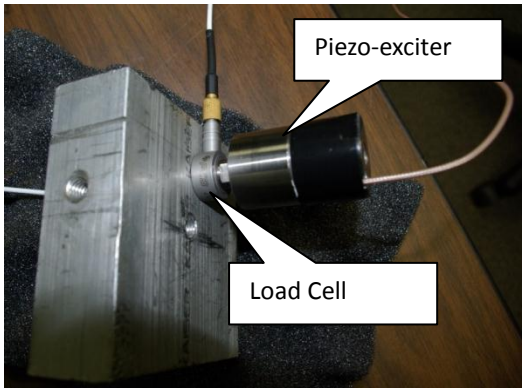

Figure 11. Mounting Method and Repeatability Test Setup, Exciter and Load Cell

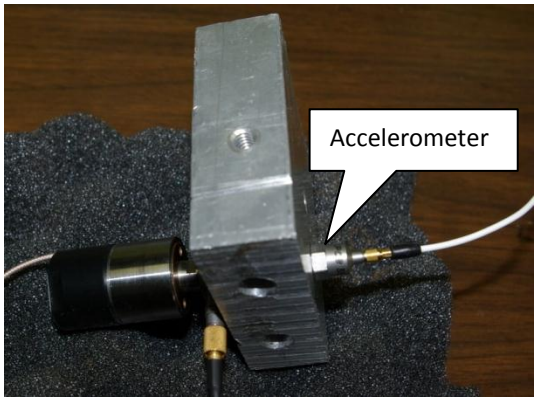

Figure 12. Mounting Method and Repeatability Test Setup, High Frequency Accelerometer

Data was recorded three times, with the test setup disassembled between tests to gauge repeatability. Note that the transducer and sensor were tightened without the use of a torque wrench and that may improve repeatability. Next, the threads for mounting the accelerometer were clearance-drilled, the accelerometer was super-glued in place, and the test was repeated three times. Between tests, the accelerometer was removed, cleaned, and re-glued; however, the piezo-exciter (with load-cell) was left in place to test just the repeatability of gluing the sensor to the surface.

The key takeaway is that the glued-accelerometer FRFs compare very well with the threaded accelerometers, so using super-glue to mount the sensors and actuator does not appreciably color the results. Figure 13 shows the average of the three threaded FRFs (blue trace) plotted with the average of the three glued FRFs (red trace). This clearly shows that the two methods are quite similar, particularly below about 40 kHz. The maximum difference between the two methods is about 8 dB (which occurs at about 47 kHz); however, for the purpose of selecting frequency bands of maximum energy transmission, this difference is unimportant.

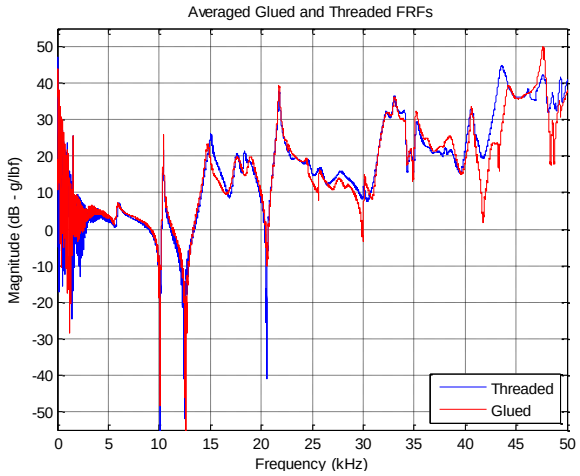

Figure 13. FRF Comparison between Threaded and Glued Accelerometer Mounting

Repeatability

Three cases of mounting and dismounting the shaker to the gearbox and comparing the resulting FRFs are shown for the bench-tested IGB in Figure 14 and an on-aircraft Blackhawk IGB in Figure 15. As can be seen, these generally match quite well – it appears that with care in mounting sensors and actuators the measurements are very repeatable. Note that the poor low-frequency response is due to the low force output with reaction-mass excitation at low frequency (discussed above).

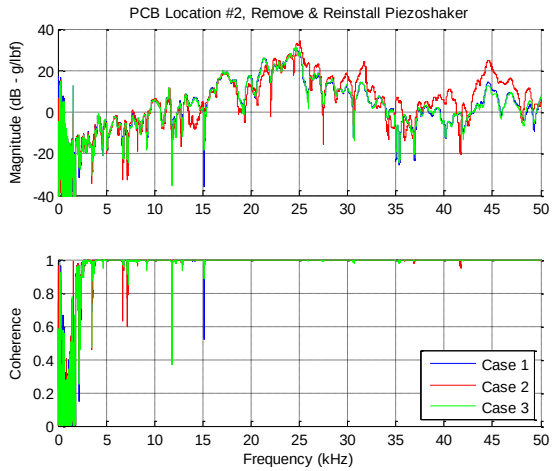

Figure 14. Repeatability of FRFs on Gearbox, Removing and Reinstalling Piezo-exciter

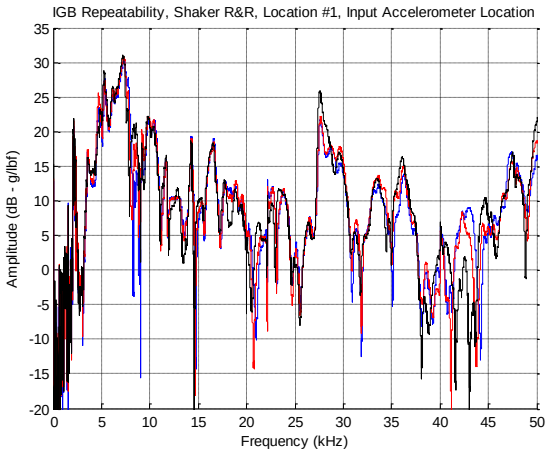

Figure 15. Repeatability of FRFs on Aircraft, Removing and Reinstalling Piezo-exciter

Again, as these tests are being performed on parked aircraft, there was some question as to whether the FRFs would change with torque applied to the drivetrain. This loads the gears and in most cases applies some radial load to the bearings, potentially altering clearances and affecting transfer path dynamics. This effect was tested in the lab on the Apache IGB; however, to be thorough, it was also tested on a complete Blackhawk. To test this on the Blackhawk, the torque was applied to both the main rotor and the tail rotor in opposite directions. This was done in both the normal direction of rotation and in the opposite direction. Figure 16 shows the results of the test on the Blackhawk – there is no appreciable difference between the FRFs.

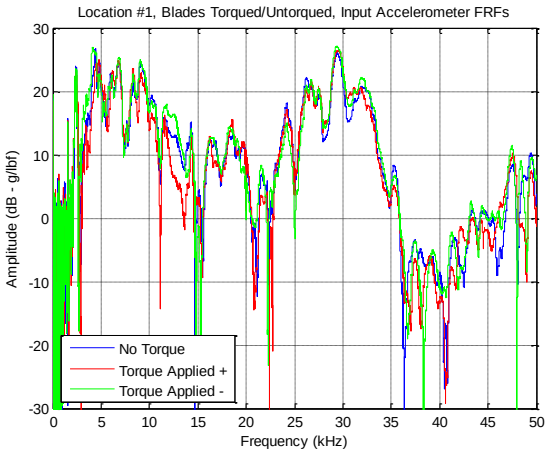

Figure 16. Drivetrain Preload – FRFs Without Preload, and with Preload in Opposite Directions, Input Accelerometer

Bearing spalling is expected to begin where the bearing load is greatest. For this reason, the transfer path from this load zone to the installed DSC sensor is what should be measured. These bearing load zones are documented in the design of each aircraft and are known to the Aviation Engineering Directorate. The information contained in the aircraft design is both

confidential to the aircraft manufacturer as well as considered official information to the government and thus it is not published as part of this paper.

Bearing load zones are not always externally accessible. This is particularly true for large planetary gearboxes, which exist on all Army aircraft. In cases where the load zone is inaccessible, the decision was made to either excite as close as reasonably possible or to excite from multiple locations near the bearing. Obviously, this technique introduces error into the recommendations made at the end of the project, but this error is significantly less than other methods of assuming the frequency response of a gearbox that has never been monitored for failure by a DSC.

Phase II and III: On Aircraft

On board results are quite comprehensive and available in several formats to the public (raw time domain and processed FRFs are both marked *For Public Release* and available by contacting the authors). For the sake of brevity, this section will present only a sample of the on aircraft data, highlighting interesting aspects of the completed study.

Hanger and Swashplate Bearings

Hanger bearings are particularly unique in both function and diagnostics recommendations. Frequently, a damper is used to reduce vibration transmitted between the airframe and the bearing. Intentionally damping the vibration between the bearing and airframe significantly changes the recommendations for bearing diagnostics computed from data collected on the airframe side of the signal. Thus sensor placement becomes the most important consideration.

Viscous damper bearings exhibited significant attenuation and a large number of anti-resonances for all excited frequencies. Figure 17 shows an example of the response for the viscous bearings on the H-60. The response is attenuated across the entire band. Current vibration diagnostics are set to look for bearing fault signatures between 13 and 18 kHz, a band that contains a noticeable drop in response near 14 kHz. The Army continues to investigate the implications of this response behavior on bearing enveloping techniques.

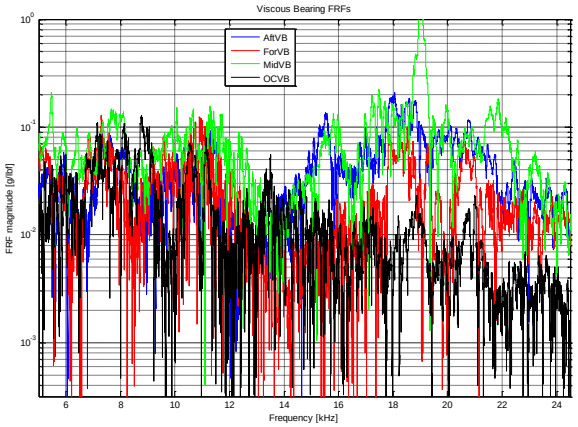

Figure 17. Example Viscous Bearing FRFs from H-60

Small gearboxes

Gearboxes where all the load zones are easily accessible from the surface and have relatively shorts paths to the DSC sensor behave in similar fashion. This includes most accessory gearboxes, tail gearboxes, engine output gearboxes, and pylon gearboxes. They represent the majority of gearboxes installed on single main rotor aircraft. Bearings closest to the sensors have fewer anti-resonances and generally exhibit amplified transmission between 10 and 20 kHz.

In a general sense, one could make the assumption that all bearing diagnostics could be set for any convenient range between 10 and 20 kHz, but to achieve the best results from the monitoring system one must account for poorly transmitting bands. While most of the

recommendations fall between 10 and 20, there are less desirable characteristics depending on individual gearboxes within the same band. For example, an intermediate gearbox might use the 15 to 20 kHz band and on the same aircraft the tail gearbox might use the 10 to 15 kHz band. If the aircraft was configured for a *blanket* value, then one would need to be sacrificed. Example small gearbox FRFs are shown in Figure 18, Figure 19, and Figure 20.

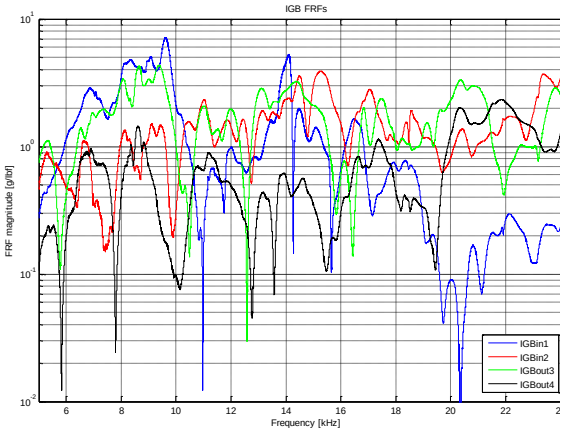

Figure 18. Example Intermediate Gearbox FRFs

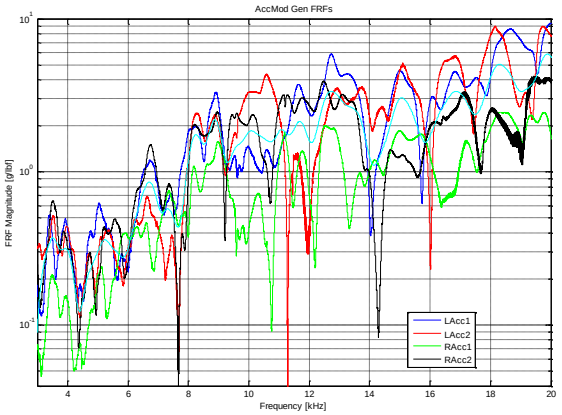

Figure 19. Example Accessory Module FRFs

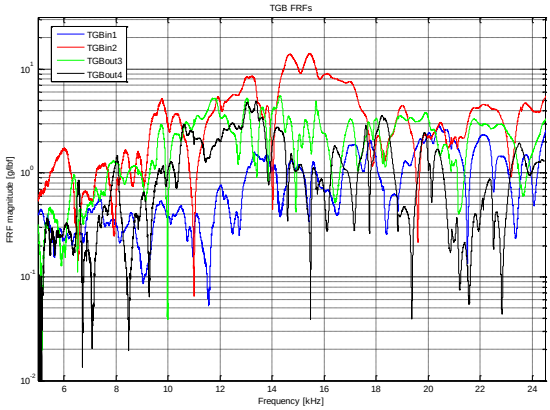

Figure 20. Example Tail Gearbox FRFs

Large gearboxes

For the purposes of this paper, large gearboxes are planetary gearboxes typically used for main rotor output power in single and tandem rotor platforms. The DSCs installed on these aircraft typically use 3 accelerometers placed at convenient locations on the gearbox for vibration diagnostics. Figure 21 shows a case when the source is ‘near’ the sensor, and Figure 22 shows a case when the source is ‘far’ from the sensor. Obviously, the response amplitude is drastically reduced when the source and accelerometer are far apart. There are also substantially more zeros in the response – the reason for this is unclear. Perhaps the greater distance traveled by the vibration stress energy through the complex structure of a helicopter transmission provides more opportunity for energy to be attenuated by various components which act as tuned-mass-dampers.

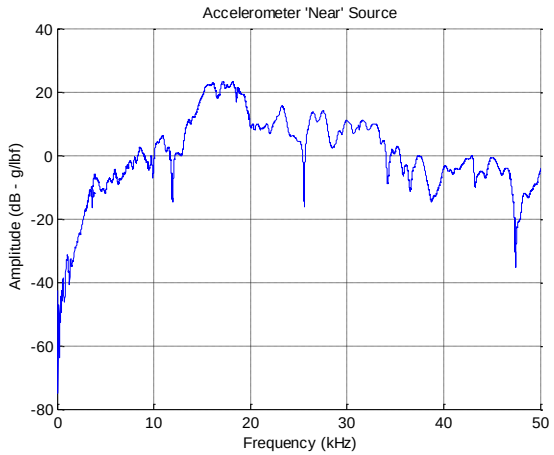

Figure 21. Shaker 'Near' Accelerometer

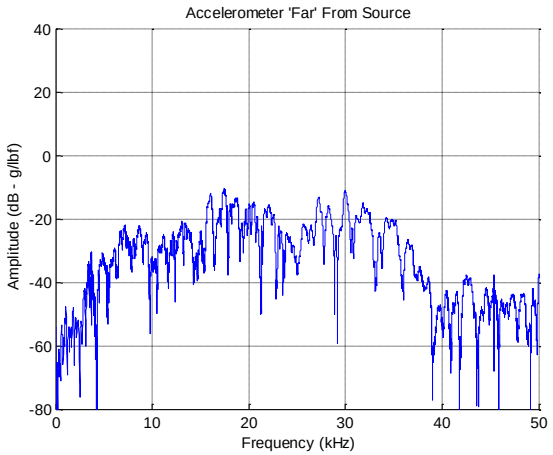

Figure 22. Shaker 'Far' From Accelerometer

Clearly, the sensor dynamics will color the measured vibration response. Figure 23 shows an example of this: the red trace is the FRF made with a DSC accelerometer, and the blue trace was made with a high-frequency accelerometer (PCB 352A60) mounted in place of the DSC sensor. The DSC sensor has a resonance at just under 35 kHz, and its response drops drastically above that frequency, while the high-frequency sensor (blue trace) shows that this drop in response is not due to the structural dynamics of the gearbox, but is instead due to the sensor's dynamics.

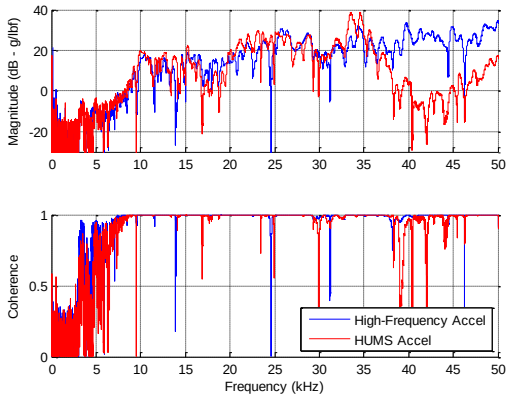

Figure 23. FRF with High Frequency Accelerometer Compared to HUMS Sensor

This study did not test the modal characteristics of the accelerometer brackets that are installed on some platforms. It is known (5) that some of the brackets used on Army aircraft have modes located in the middle of accelerometer (manufacturer calibrated) linearity regions. This is an effect that must be better understood if improved bearing vibration diagnostics are to be obtained by the Army and it is recommended that further study of the data focus on improving Condition Indicators by avoiding potential transfer path pollution. This is particularly salient for the case of extending bearing life based on vibration based diagnostics.

Damping

The damping in the vibration transfer paths measured during this testing is higher than expected. Use of the half power method for damping estimation has shown that for any gearbox, damping ratios of the highest amplitude modes range from 1% to more than 50%. This result has led AED to begin a study that examines the relationship between enveloping, broadband noise, and CI behavior as a function of damping ratio. This is being examined as a function of a single degree of freedom, as well

as multiple degrees of freedom. A critical question for future vibration diagnostic development will focus on this relationship.

Conclusions

The Frequency Response Functions between expected bearing spall initiation sites and installed DSC accelerometers has been measured for four different US Army aircraft models: the Black Hawk, the Chinook, the Kiowa Warrior, and the Apache. The process for verifying and validating that surface excitation can be used to estimate FRFs was presented. The results of this study can be used to set vibration signal demodulation windows in Health and Usage Monitoring Systems.

Future Work

Is it possible to measure a dynamic FRF during aircraft operation? Preliminary work in this area has been considered. At this time, the authors are considering a small study on a test stand to demonstrate the measurement of dynamic FRFs in an environment that includes significant noise sources. The authors are interested in the potential changes caused by the noise and structure.

Damping and its influence on CI behavior needs to be well understood and is being actively addressed by the AED.

Acknowledgements

This dataset would have never been collected if not for the efforts of Army aviators located at Ft Rucker, Ft Campbell, and Redstone Arsenal; your service and assistance is appreciated. The authors would like to thank Jeremy Partain, James Hunt, Jeremy Branning, Lance Sweeley, Lance Antolick, Rick Roth, and Stu Shelley for their assistance in collecting such a large dataset. The funding for this effort was provided by the efforts of Gail Cruce and Jeff Bagwell.

References

1. *Comparison of Test Stand and Helicopter Oil Cooler Bearing Condition Indicators.* **Dempsey, Paula J, et al.** Phoenix AZ : American Helicopter Society Forum 66, 2010. AHS.

2. *Examples of Condition Based Maintenance with the Vibration Management Enhancement Program.* **Keller, Jonathan A, et al.** Grapevine TX : American Helicopter Society Forum 61, 2005. AHS.

3. **Norton, Michael Peter and Karczub, Denis G.** *Fundamentals of Noise and Vibrations Analysis for Engineers.* Cambridge : Cambridge University Press, 2003.

4. **Kamen, Edward W. and Heck, Bonnie, S.** *Fundamentals of Signals and Systems Using the Web and MATLAB.* Upper Saddle River : Pearson Prentice Hall, 2007.

5. *A Vibration Study on a Health Usage and Monitoring System Accelerometer Mount in the Time, Frequency, and Modal Domains.* **Hochmann, David, et al.** Montreal : American Helicopter Society Annual Forum 58, 2002. AHS.